An Optimized Fiber Delivery System for Q-switched, Nd:YAG Lasers

Robert E. Setchell

Sandia National Laboratories, MS1421
Albuquerque, New Mexico 87185

ABSTRACT

Interest in the transmission of high intensities through optical fibers is being motivated by an increasing number of applications. Using different laser types and fiber materials, various studies are encountering transmission limitations due to laser-induced damage processes. For a number of years we have been investigating these limiting processes during the transmission of Q-switched, multimode, Nd:YAG laser pulses through step-index, multimode, fused-silica fiber. We have found that fiber transmission is often limited by a plasma-forming breakdown occurring at the fiber entrance face. This breakdown can result in subtle surface modifications that leave the entrance face more resistant to further breakdown or damage events. Catastrophic fiber damage can also occur as a result of a variety of mechanisms, with damage appearing at fiber entrance and exit faces, within the initial "entry" segment of the fiber path, and at other internal sites due to fiber fixturing and routing effects. System attributes that will affect breakdown and damage thresholds include laser characteristics, the design and alignment of laser-to-fiber injection optics, and fiber end-face preparation.

In the present work we have combined insights gained in past studies in order to establish what thresholds can be achieved if all system attributes can be optimized to some degree. Our multimode laser utilized past modifications that produced a relatively smooth, quasi-Gaussian profile. The laser-to-fiber injection system achieved a relatively low value for the ratio of peak-to-average fluences at the fiber entrance face, incorporated a mode scrambler to generate a broad mode power distribution within the initial segment of the fiber path, and had improved fixturing to insure that the fiber axis was collinear with the incident laser beam. Test fibers were from a particular production lot for which initial-strength characteristics were established and a high-stress proof test was performed. Fiber end faces were prepared by a careful mechanical polishing schedule followed by surface conditioning using a CO_2 laser. In combination, these factors resulted in higher thresholds for breakdown and damage than we had achieved previously in studies that utilized a simple lens injection system. Probability distribution functions were fitted to the threshold data, providing a means for estimating the probability for transmission failure at lower laser energies.

Keywords: high-intensity fiber transmission, laser damage in optical fibers

1. INTRODUCTION

Applications that are currently motivating interest in high-intensity laser transmission through optical fibers include certain medical procedures,[1,2] laser acceleration of flyers for studies of material behavior under impulsive loading,[3,4] and prompt initiation of secondary explosives using methods inherently safe from accidental electrical currents.[5,6] As laser intensities within a fiber are increased, however, transmission will eventually be interrupted by laser breakdown or laser-induced damage. Our studies of these events have been limited to the case of Q-switched, multimode, Nd:YAG laser pulses at the fundamental wavelength (1.064 μm) transmitted through step-index, multimode, fused silica fiber. A number of breakdown and damage processes have been identified, as illustrated in Fig. 1. Of these various processes, we have found that fiber transmission is often limited by a plasma-forming breakdown at the fiber entrance face. In this process, subtle surface modifications can occur that leave the fiber face more resistant to further breakdown or damage events. We denote this process as breakdown rather than damage to distinguish it from plasma-forming events on the entrance face in which small pits form on the surface, and subsequent laser pulses simply produce more violent events with more extensive pitting. The other catastrophic damage processes that are possible can result in damage appearing at the fiber exit face, within the initial "entry" segment of the fiber path, or at other internal sites due to fiber fixturing and routing effects.[7-11]

For a given laser and fiber configuration, we have found that the particular breakdown or damage mechanism that will dominate and its corresponding threshold will generally depend on the following system attributes: laser characteristics,

DISCLAIMER

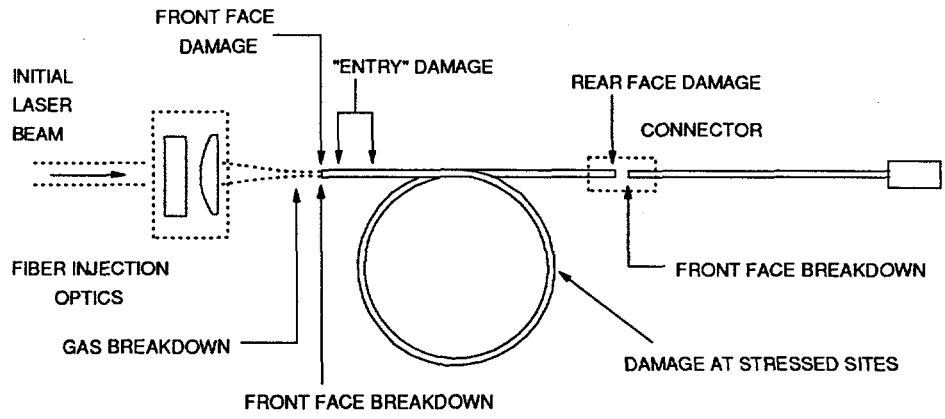

Fig. 1 Breakdown and damage processes in a high-intensity fiber transmission system

the design and alignment of laser-to-fiber injection optics, and fiber end-face preparation. Entrance-face breakdown and damage depend on the surface characteristics resulting from the end-face preparation process, and on the peak fluences at this face resulting from the laser characteristics and the design of the laser-to-fiber injection optics. Previous studies examined how entrance-face thresholds can be affected by end-face preparation techniques such as different mechanical polishing schedules,[7] adding CO_2-laser conditioning following mechanical polishing,[9] and cleaving.[10] A particular schedule for CO_2-laser conditioning following an optimized mechanical polishing schedule was found to produce surfaces very resistant to breakdown.[9] The other factor determining entrance-face thresholds is the relation between peak fluence at this surface and the incident energy. By the use of magnified beam-profiling techniques, the actual fluence distribution on a fiber entrance face resulting from a particular combination of laser and injection optics can be established. One figure of merit for laser conditions at the entrance face can be defined by the following ratio of peak-to-average fluences:

$$P/A = \frac{\text{peak local fluence}}{(\text{total energy incident on fiber core})/(\text{fiber core area})}$$

We try to confine the incident laser energy to the fiber core to prevent energy from propagating in the cladding. A perfect "flat top" fluence distribution extending over the entire core area would achieve a value of unity for this ratio. In practice, using different lasers and injection optics, we have achieved values for this ratio varying from less than 3 to more than 5. The highest values have resulted from multimode lasers with very strong "hot spots".

Damage beyond the entrance face but within the initially straight portion of the fiber path is denoted as "entry" damage. This damage occurs when initial reflections along the core/cladding interface result in internal beam focusing, with very high fluences produced within one or more fiber cross sections in this region. In general, a great many reflections over a considerable length of fiber are necessary before a reasonably steady fluence distribution is established in fiber cross sections.[12] When "entry" damage dominated the results in one previous study,[8] examination of the beam profiles from our multimode laser at the fiber entrance face and beyond showed very strong, persistent "hot spots." This led to modifications of our test laser to produce smooth, quasi-Gaussian profiles in both the near field and far field.[9] Even with a laser having a relatively benign spatial profile, however, "entry" damage can be easily introduced. Early studies[13-15] found that the laser axis and the initial fiber axis need to be collinear to avoid this damage process. In addition, these studies found that the fiber entrance face should be positioned beyond the focal plane of the injection lens so that the beam will be diverging as it enters the fiber. A larger divergence angle, as will occur with an injection lens having a shorter focal length, helps to inhibit the damage process.

Assuming that the laser and fiber axes are collinear and the laser beam is reasonably axisymmetric, the divergence and intensity distribution of the beam entering the fiber entrance face define the initial mode power distribution (MPD) within the fiber. The MPD is a description of how the total laser power is distributed with respect to the angle that rays make with the fiber axis.[12] The maximum possible angle is the critical angle for total internal reflection. Unless an injection lens with

a very short focal length is used, the initial mode power distribution may only extend over angles much smaller than the critical angle. In addition to enhancing "entry" damage, this condition can lead to a persistent damage mechanism within the first major bend along the fiber path. In one previous study, internal damage was consistently observed within a fiber segment that transitioned from a straight entrance path to a constant-radius bend that continued through 360°. The cause of this damage was determined to be very high fluences in the outside portion of the fiber cross section (away from the center of curvature).[11] Although any bend in the fiber path will cause the mode power distribution to become asymmetric, the extreme asymmetry in this case was due to a significant portion of the total energy being confined to "whispering gallery" rays[16] that only reflect from the outer core/cladding boundary. To inhibit this damage process, the mode power distribution must be broadened prior to the first bend in the fiber path. This requires either innovative injection optics or mechanical mode mixing in the entrance segment.

An additional damage mechanism has been observed in previous studies at positions along the fiber path where the path was forced to experience a small bending radius locally. Such a condition can be introduced inadvertently when a fiber is routed around a thin post or sharp edge and then some axial tension is applied. This is especially easy to do if the fiber only has a thin buffer and no additional protective layers. In a few cases a measurable loss in transmission was noted before damage, indicating that the locally imposed bend was causing some of the laser energy to exceed the critical angle for total internal reflection and pass through the cladding into the buffer. In other cases no loss in transmission was observed prior to damage, suggesting that the locally imposed geometry was causing focusing within the fiber core. In some of these cases the damage did not occur immediately, which prompted an investigation into possible time-dependent mechanisms.[11] Damage related to local path aberrations can also result from fiber fixturing. In one study, careless fixturing of an array of fibers resulted in every fiber damaging at nearly the same location behind the fixture at relatively low energies.[8] Use of a high-shrinkage epoxy apparently caused the path of each fiber to be locally distorted exiting the fixture. These examples illustrate that this particular damage process can be avoided if sufficient care is taken in the handling, routing, and fixturing of fibers.

The damage mechanism at the fiber exit face is quite different from that at the entrance face. Assuming that a reasonably good surface finish has been achieved through polishing, damage at this face will typically result from subsurface defects remaining from early polishing steps.[7] We have also observed exit face damage with cleaved surfaces, possibly due to subsurface fractures created during the cleaving process. This dependence on subsurface features for exit face damage results from a standing wave pattern during the laser pulse that produces peak intensities at discrete depths into the silica.[17] Exit face damage typically results in one or more large craters that start from the depth where the damage initiates. Subsurface defects are difficult to detect and can be present even if the final surface finish is very good. Minimizing this form of damage depends on developing a careful polishing schedule in which sufficient material is removed at each step.

Although all of our studies have used multimode Nd:YAG lasers, certain issues can be identified if fiber transmission is under consideration for other high-power lasers. Relevant laser characteristics can be divided into three areas: basic parameters (wavelength and pulsewidth), transverse mode characteristics, and spectral linewidth. Threshold fluences for breakdown and damage generally decrease with decreasing wavelength and pulsewidth.[18] Elimination of strong "hot spots" in multimode lasers through design and alignment has been mentioned previously as a means of inhibiting entrance-face breakdown and "entry" damage. Concerns introduced by the use of a TEM_{00} laser beam include breakdown or damage at a focus within the laser-to-fiber injection segment, "entry" and initial-bend damage due to a narrow initial MPD generated in the fiber, and the onset of nonlinear effects within the fiber. The spectral linewidth of a laser depends on the number of axial cavity modes active within the lasing medium's gain profile. A smaller linewidth corresponds to greater temporal coherence, which enhances interference between propagating modes in a multimode fiber. The intensity distribution across the exit face of relatively short fibers (a few meters) can then have strong interference maxima and minima,[9] which may be undesirable for some applications. For longer fiber paths (tens of meters) a smaller spectral linewidth will result in earlier onset of nonlinear effects, particularly stimulated Brillouin scattering.[19]

In the present study we have tried to establish what thresholds could be achieved with a laser delivery system in which all of the important system attributes have been optimized to some extent. The next section describes the resulting experimental configuration. The following section describes the methods used for conditioning fiber faces with a CO_2 laser. Subsequent sections present and discuss the threshold data obtained with the current system.

2. CURRENT EXPERIMENTAL CONFIGURATION

The experimental configuration used in the present study is shown schematically in Fig. 2. The test laser is a compact, oscillator-only, multimode Nd:YAG (Laser Photonics Model YQL-102) operated at the fundamental wavelength (1.064 μm) in a Q-switched, single-shot mode. In a previous study[9] the alignment of this laser was altered to produce nearly Gaussian

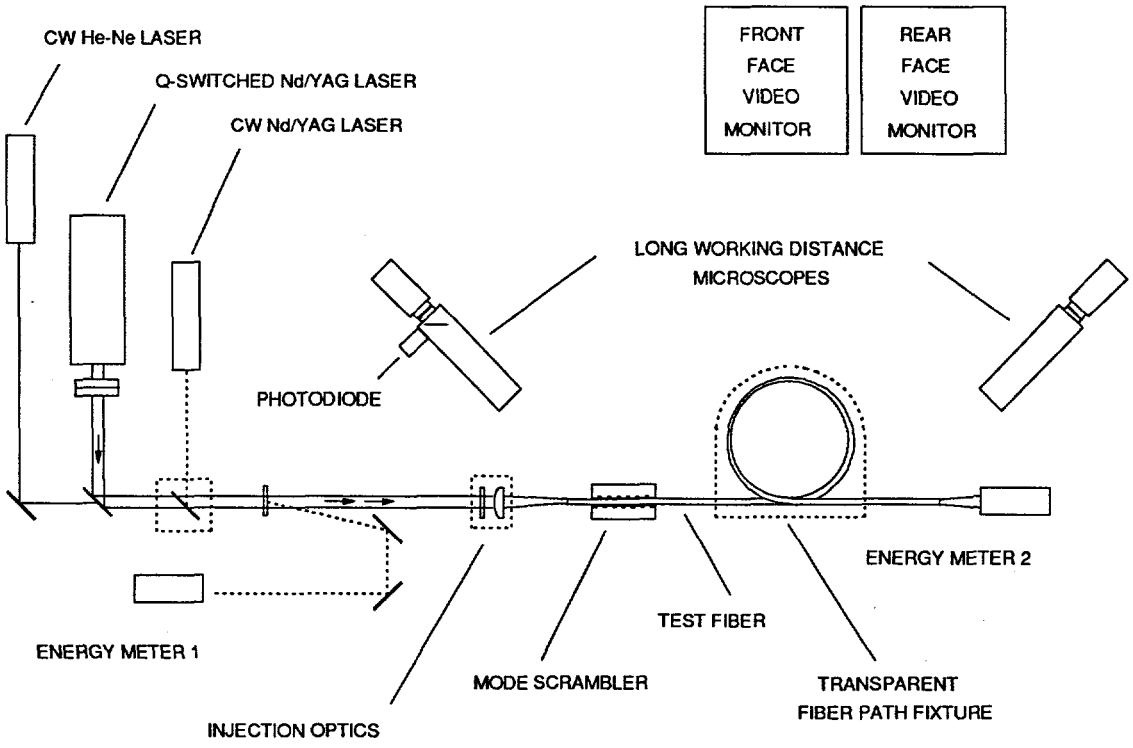

Fig. 2 Experimental configuration for fiber damage testing

near-field and far-field profiles while preserving its full multimode output energy. Typical near-field profiles are shown in Fig. 3. For the present study an additional regulated heat exchanger was added to the laser cooling system to ensure output consistency over extended periods of operation. The laser pulsewidth (FWHM) is now 13.5 ± 0.5 ns, as shown in Fig. 4. A single plano-convex lens having a 50-mm focal length was used to inject the laser beam into the fiber entrance face, which was positioned a few millimeters beyond the focal plane. The distance from the lens to the entrance faces of successive test fibers was carefully repeated (to within ± 50 μm) to minimize variations in test conditions. A magnified beam-profiling

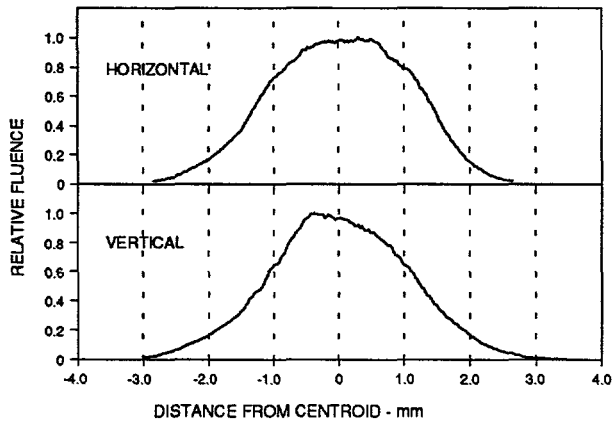

Fig. 3 Laser near-field beam profiles

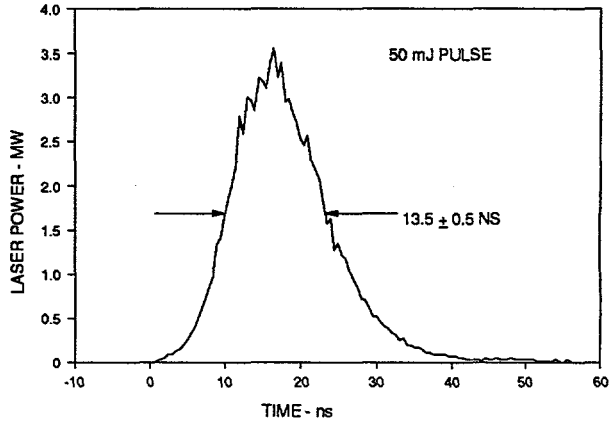

Fig. 4 Laser temporal profile

system was used to determine the actual fluence distribution at the entrance-face location, as shown in Fig. 5. As in the laser near-field profile (Fig. 3), a smooth, quasi-Gaussian distribution exists at the fiber face. The magnified beam profiles also provide a measurement of the ratio of peak-to-average fluences at this location (as defined previously). In the current study the average value for this ratio was 3.09, with a standard deviation of 0.14 (as determined from 120 single pulses). The initial portion of the fiber path was held in a custom fixture designed to improve our ability to align the fiber axis parallel to the laser axis. This fixture also had orthogonal micrometer drives for centering the fiber axis on the laser axis through active alignment at a low laser energy. The fiber entrance and exit faces were observed during testing with long-working-distance video microscopes. A more sensitive means of detecting entrance-face breakdown was achieved by directing some of the light entering this video microscope into a photodiode. A filter blocked scattered laser light, and broad-band breakdown emission produced signals that were recorded on a digital oscilloscope. A CW He-Ne laser was operated collinearly with the Nd:YAG laser to enhance detection of end-face and internal damage.

All the fibers used in the present study were type FG-365-UER from a single production lot at 3M. These fibers have a 365-μm diameter core of high-OH^- fused silica, a 17.5-μm thick cladding of F-doped fused silica (resulting in a numerical aperture of 0.22), a 15-μm thick TECS™ coating, and a 150-μm thick Tefzel® buffer. Instead of the standard 100 kpsi proof test normally conducted on production fiber, 3M subjected all of our fiber to a 250 kpsi proof test under uniform tension. In addition, a portion of the same production lot was used for dynamic strength testing to establish a Weibull statistical distribution for failure probability versus applied stress.[20] Such a distribution is in the form:

$$F(\sigma) = 1 - \exp(-\sigma / \sigma_0)^m$$

where $F(\sigma)$ is the cumulative probability for failure at stress σ, m is the Weibull slope, and σ_0 is a scale parameter. Values of m and σ_0 for this lot of fiber were found to be 146.4 and 736.0 kpsi, respectively. These values are quite large, indicating a very high-quality fiber having only a narrow distribution of very small surface flaws.[20]

An optimum laser-to-fiber injection system would mitigate any "hot spots" in the beam to produce a smooth fluence distribution over most of the fiber entrance face, would be relatively insensitive to alignment errors, and would immediately generate a broad mode power distribution in the fiber without any regions of internal focusing. In other words, optimum beam characteristics at the fiber entrance face would essentially be the same as would be found at a fiber exit face after a lengthy propagation distance. Conventional optics are not likely to provide these features. In one previous study a diffractive optical element was evaluated as a component in the laser-to-fiber injection optics.[10] Although this element was successful in achieving the intended intensity distribution at the fiber entrance face, it produced a focused pattern at some depth into the fiber that resulted in early damage. Since then we have evaluated two more diffractive elements that have been designed and fabricated at Sandia National Laboratories for use in laser-to-fiber injection optics. Each design has been an improvement over prior elements, but to date a completely satisfactory design has not been achieved. Consequently, in the present study a simple lens approach was still used to inject the beam into the fiber. However, a mechanical mode scramber was added to the initial fiber path in order to generate a broader mode power distribution. A sketch of this device is shown in Fig. 6. The top and bottom pieces each hold a series of cylindrical rods 1.2 mm in diameter that protrude out

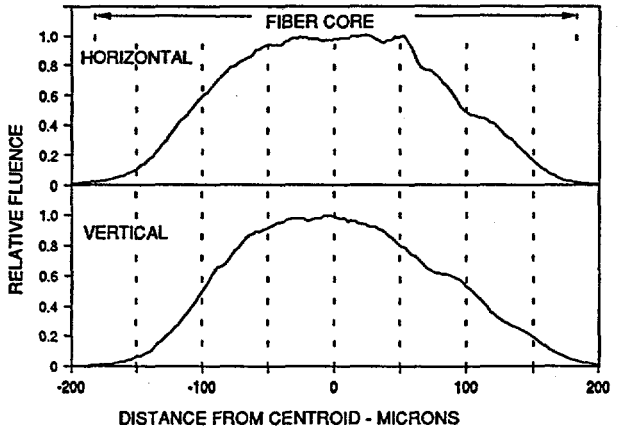

Fig. 5 Laser beam profiles at the fiber entrance face

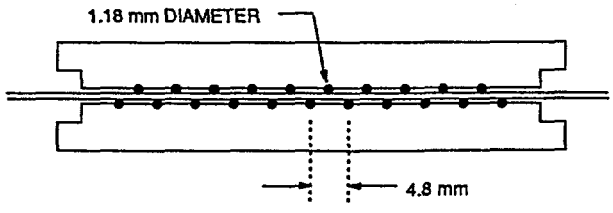

Fig. 6 Mode scrambler fixture

from the mounting surface approximately 0.4 mm. With a test fiber in between, the top and bottom pieces are brought together against a hard stop that leaves a 0.60-mm gap between the top and bottom rods. The total fiber diameter is 0.73 mm, but this includes a 0.30-mm total thickness of fairly compressible Tefzel. The actual deflection of the fiber axis within this device has not been determined, but it is certainly less than the 50-70 μm microbend deflections examined in a previous study[10] which resulted in transmission losses of 5-45%. Transmission losses for the design shown in Fig. 6 were less than 2%. Figure 7 shows the effect of the mode scrambler on fluence profiles across the fiber core at a location within a bend. The techniques used to obtain such a profile were described previously.[11] Without the mode scrambler the profile is strongly shifted to the outside of the bend, resulting in the ratio of peak-to-average fluences having a value of 4.4. With the mode scrambler the profile is more uniform across the fiber core, with the ratio of peak-to-average fluences falling to 2.1. The mode scrambler has very little effect on the fluence distributions at the fiber exit face, as shown in Fig. 8. The intensity variations shown in Figs. 7 and 8 are due to interference between fiber modes, as mentioned in the previous section.

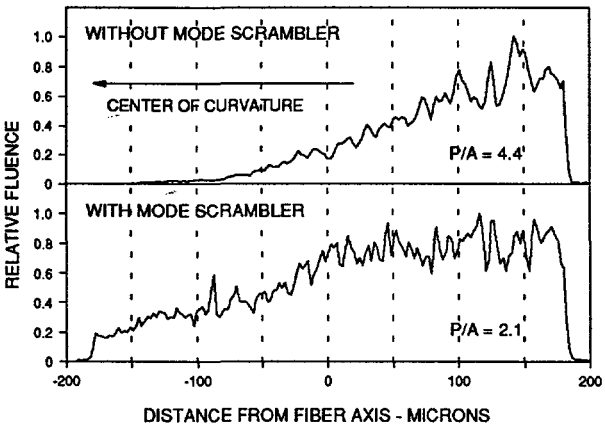

Fig. 7 Effect of mode scrambler on fiber near-field profile at a position 24° beyond the start of a bend with a constant 7.5-cm radius

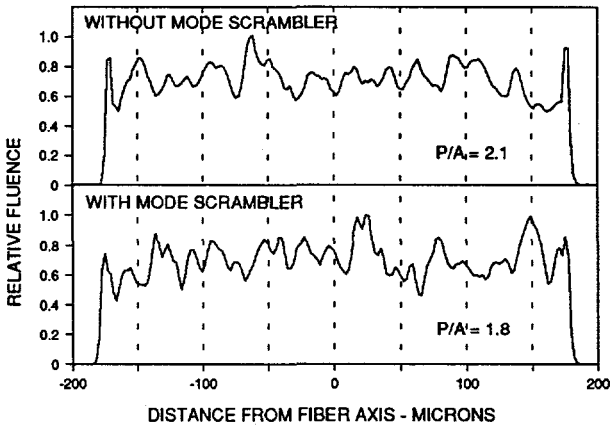

Fig. 8 Effect of mode scrambler on fiber near-field profile at the fiber exit face

3. CONDITIONING OF FIBER END FACES USING A CO_2 LASER

In a previous study[9] a significant improvement in entrance-face breakdown thresholds was achieved when fiber end faces were conditioned with a CO_2 laser using a particular conditioning schedule. A different schedule was found to have a detrimental effect on measured thresholds. These contrasting results were consistent with earlier studies on CO_2-laser conditioning of bare fused-silica surfaces.[21,22] For the current study, a new system for CO_2 laser conditioning of fiber end faces was assembled. This system is shown schematically in Fig. 9. The CO_2 laser is a Synrad Model 48I-1 having a

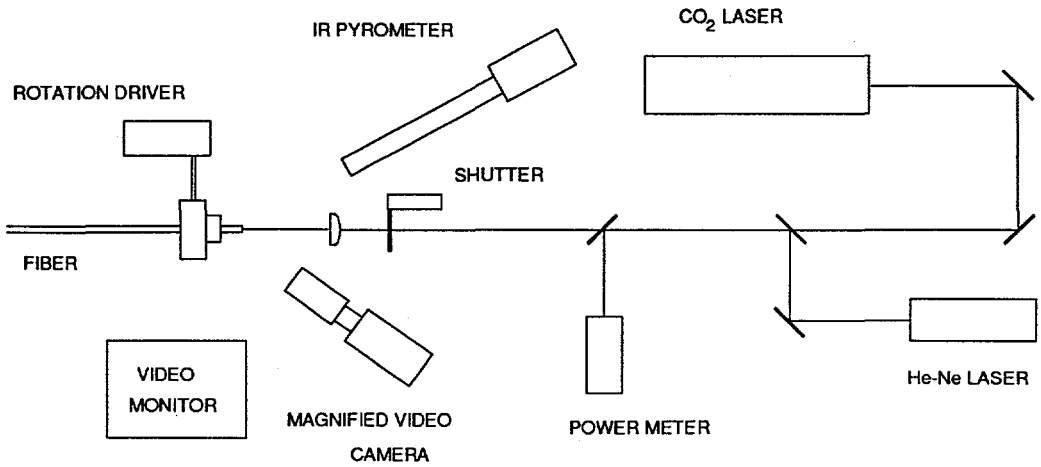

Fig. 9 Configuration for conditioning fiber faces with a CO_2 laser

maximum CW output of 7.5 watts. Fibers were held in a fixture that rotated at 6 rpm, with the end faces held a fixed distance beyond the focal plane of a focusing lens. The end face was observed with a magnified video camera and an IR pyrometer that was custom made for this application by Vanzetti. Because of temperature variations across the fiber face, the pyrometer provided only a qualitative measure of surface temperatures. Signals from the pyrometer and a meter monitoring the laser power were recorded digitally for each fiber. An electric shutter was used to expose the fiber end face to a constant incident laser power for a fixed 30-second duration. Figure 10 shows the Gaussian intensity distribution on the fiber end face during this exposure. This distribution was determined by measuring the fraction of incident power transmitted by small apertures positioned at the same location. Figure 11 shows side-on profiles of fiber end faces measured before and after the conditioning process. The incident laser power and the exposure time were selected to match the degree of rounding near the edge (within the cladding) that had resulted from the most successful conditioning schedule found in the previous study.

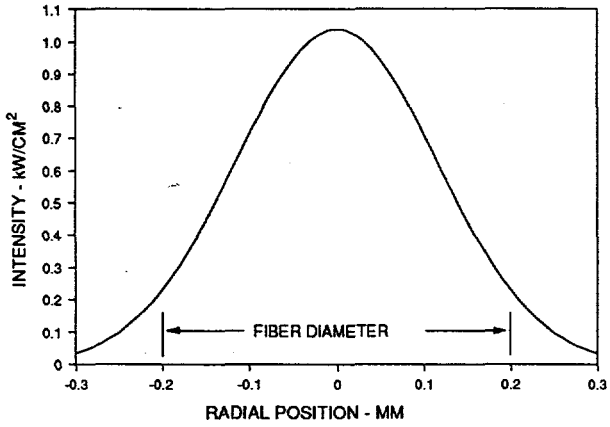

Fig. 10 The CO_2 laser intensity distribution on the fiber face

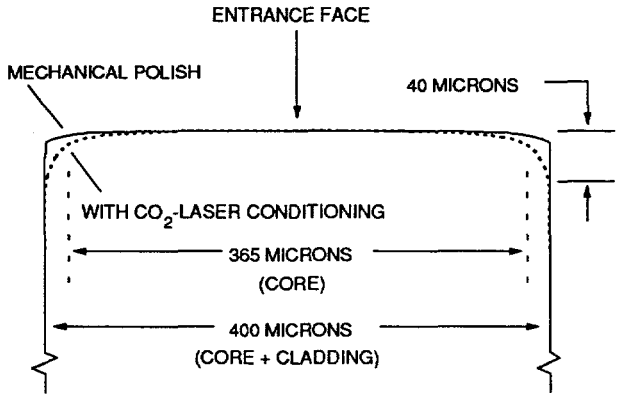

Fig. 11 The effect of CO_2-laser conditioning on the shape of the fiber face

4. RESULTS

The test procedure used for each fiber is illustrated in Fig. 12. After alignment using very low pulse energies, the fiber is subjected to a series of single laser pulses in which the incident energy is increased with each successive pulse. The testing is halted when a breakdown or damage event occurs on a given shot, as determined by some combination of the entrance-face breakdown detector, the appearance of scattered He-Ne laser light, and the measured fiber transmission. For simplicity the term "damage" will now be used to indicate the first breakdown or damage event that occurs during the test procedure. The maximum energy transmitted before damage, together with the attempted and actual transmitted energies at damage, were then recorded. In past studies, such results were presented in terms of the percentage of a given lot of test fibers that transmitted certain energy levels before a breakdown or damage event occurred. In the current study, probability distributions were fit to the test results to provide a means for estimating damage probabilities at lower laser energies.

In order to establish the relative value of the end-face conditioning process using the CO_2 laser, we initially tested a number of fibers for which this conditioning process was omitted. The results, shown in Fig. 13, are presented in terms of cumulative damage probability versus the maximum transmitted energy before damage. To represent the results in this fashion, the individual fiber results were first ordered from lowest to highest transmitted energy E_i before damage, then assigned a corresponding rank R_i, where R_i = 1,2, 3 .....N (N is the total number of fibers tested). The cumulative probability for damage F_i at energy E_i was then assigned according to:[23]

$$F_i = (R_i - 0.5)/N$$

A Weibull distribution in terms of the variable E_i was obtained from a least-squares fit to the function:

$$F(E) = 1 - \exp(-E/E_0)^m$$

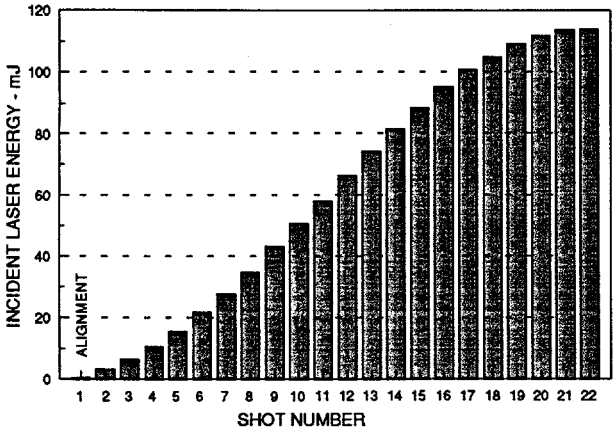

Fig. 12 Fiber test sequence

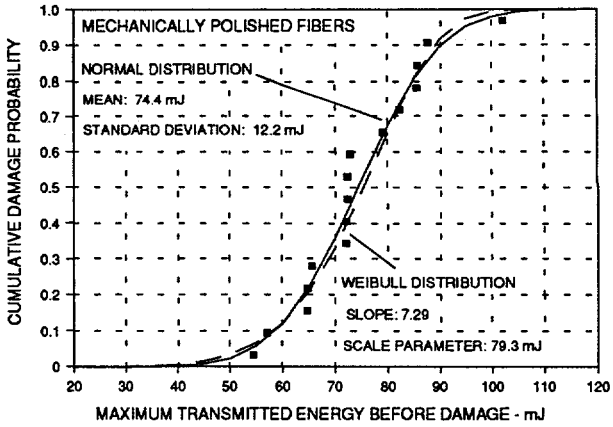

Fig. 13 Initial test results with mechanically polished fibers

where the Weibull slope m and scale parameter E_0 were introduced in a previous section. Weibull distributions are commonly used to characterize the strength of brittle materials, in which the most serious flaw in the sample is assumed to control the strength. The most serious flaw may not be the largest, but will be where the combination of flaw size and local stress results in the largest stress intensity factor. This appears to be a good analogy to laser-induced damage in fibers, where damage thresholds will be controlled by sites where the combination of defect absorption and laser intensity is most severe. For comparison with the Weibull distribution, a normal distribution was obtained from the mean and standard deviation of the E_i values. The Weibull distribution is more conservative, giving higher damage probabilities at lower energies than the normal distribution.

Figure 14 shows the results obtained with fibers that had end faces conditioned with the CO_2 laser. Compared to the results in Fig. 13, the cumulative probability distribution is shifted to higher transmitted energies by approximately 15 mJ, and the distribution width is slightly narrower. Additional comparisons between these results will be made in the following section. Another representation of the results with CO_2-laser conditioning is shown in Fig. 15. Instead of transmitted energy, cumulative damage probability is shown versus the peak fluence incident on the fiber face before damage. This form permits comparisons with non-fiber data, as peak incident fluence is the typical measure for representing damage characteristics at surfaces.[18] In Fig. 5, the relative variation of fluence over the fiber entrance face was shown for a typical laser pulse. From such profiles the ratio of peak-to-average fluences at this face can be determined. With this ratio, measured energies can be converted directly to peak incident fluences. However, shot-to-shot variations in the laser's multimode output will result in similar variations in the value of this ratio. A number of individual beam profiles were recorded (a total of 120 over several days and under different operating conditions) in order to establish mean and standard deviation values for this ratio. The central curve in Fig. 15 shows the distribution obtained using the mean value of this ratio to convert from measured energies to peak fluences. The adjacent curves show the distributions obtained using a value for the ratio equal to the mean value plus or minus one standard deviation. The span of these curves indicates the uncertainty in peak fluence values using our particular test laser.

5. DISCUSSION

The goal of the present study was to establish what thresholds for laser-induced breakdown and damage could be achieved if all of the important system attributes could be optimized to some degree. However, one of these attributes was not as optimal as had been achieved in a previous study. A fiber-to-fiber injection method used a few years ago[9] was clearly the most benign injection technique devised to date. In this approach, the test laser was injected into a 2-meter length of "conditioning" fiber using the same simple lens as used in the current study. This "conditioning" fiber had a larger diameter and a smaller numerical aperture than the fibers that were tested for damage thresholds, and was arranged with two 25-cm diameter loops along its path to encourage mode mixing. Because of the larger diameter, peak fluences at the entrance face were substantially lower than at the entrance face of the test fibers. Two lenses were used at the fiber exit to image its output onto the entrance face of a test fiber. Because the "conditioning" fiber had a lower numerical aperture (0.11 in comparison to 0.22 for the test fibers), the output could be demagnified sufficiently to fit within the core of the test

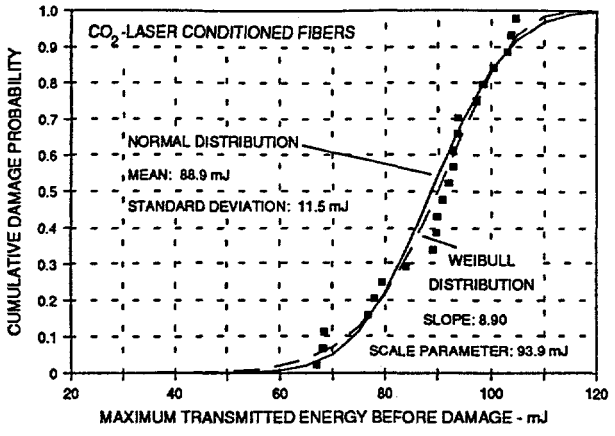

Fig. 14 Test results using fibers conditioned with a CO_2 laser

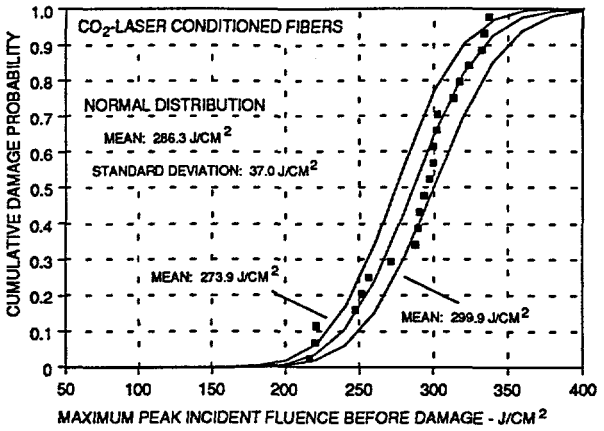

Fig. 15 Test results in terms of peak fluence incident on the fiber entrance face

fibers without exceeding their numerical aperture. This arrangement came reasonably close to an ideal injection condition in which beam characteristics at the entrance face are essentially the same as would be found at the exit face after a long fiber path. Unfortunately, applications of interest are restricted in terms of the space available for the injection optics, and this method has not been utilized recently.

Figure 16 shows comparisons between the present results, the previous results obtained with the fiber-to-fiber injection method, and some previously unreported measurements of interest. Instead of probability distributions, the curves in this figure represent the percentage of fibers within a particular test lot that reached certain levels of peak incident fluence before a breakdown or damage event occurred. Measured mean values for the ratio of peak-to-average fluences at the entrance face were used to find peak incident fluences from measured energies. Curves 2 and 5 were obtained with the fiber-to-fiber injection method using fibers having a very good mechanical polish and fibers also having end faces conditioned with a CO_2 laser, respectively. This injection method obviously inhibited internal damage mechanisms, for the only breakdown or damage mechanism observed in these tests was entrance-face breakdown. The current test procedure extended to higher fluences than were achieved in the earlier study, and the results are shown by curves 6 and 7. The mechanically polished fibers (curves 2 and 6) compare closely, whereas the current results for fibers having end faces conditioned with a CO_2 laser are not quite as good as the earlier results. For comparison, some previously unreported measurements are also included in Fig. 16. Curves 1 and 4 show results obtained with fiber having either polished or cleaved end faces as received from a commercial vendor. The commercial polish (curve 1) was clearly inferior, but the cleaved surfaces (curve 4) were exceptionally resistant to entrance-face breakdown. This contrasts with an earlier study using commercially cleaved fibers (curve 3), although this earlier lot may have had some form of end-face contamination that we were not able to remove prior to testing. The fibers used for curves 1 and 4 were much larger in diameter than in the present study, but the beam profile at the entrance face of these large fibers was comparable in size (Fig. 5). Consequently, the ratio of peak-to-average fluences at the entrance face was very high, and breakdown or damage only occurred at this position. If all of our prior test results are taken into consideration, the present test configuration produced higher thresholds for breakdown and damage than had been achieved in all previous studies that utilized a simple lens injection system.

A common definition of damage threshold is the highest tested fluence at which no damage events are observed. Applying this definition to the current study would result in thresholds in terms of peak incident fluence of approximately 185 J/cm^2 for fibers without CO_2-laser conditioning and 215 J/cm^2 for fibers with conditioning (Fig. 16). However, this definition is often applied within the context of "one-on-one" testing, where a number of different sites on a sample are tested with one incident pulse at a given fluence. The fraction of sites damaging at this fluence is recorded, then a number of new sites are tested in the same fashion at a different fluence. Over some range of fluence values, the fraction of damaging sites will vary from zero to unity. This approach is clearly impractical with optical fibers, leading to the procedure in which single laser pulses are passed through the fiber at progressively higher energies (Fig. 12). Thresholds obtained in this manner are really "conditioned" results since sub-threshold laser fluences may have affected defects in such a way as to make them more resistant to damage.[24] In addition, the laser spot size at the fiber entrance face is much smaller

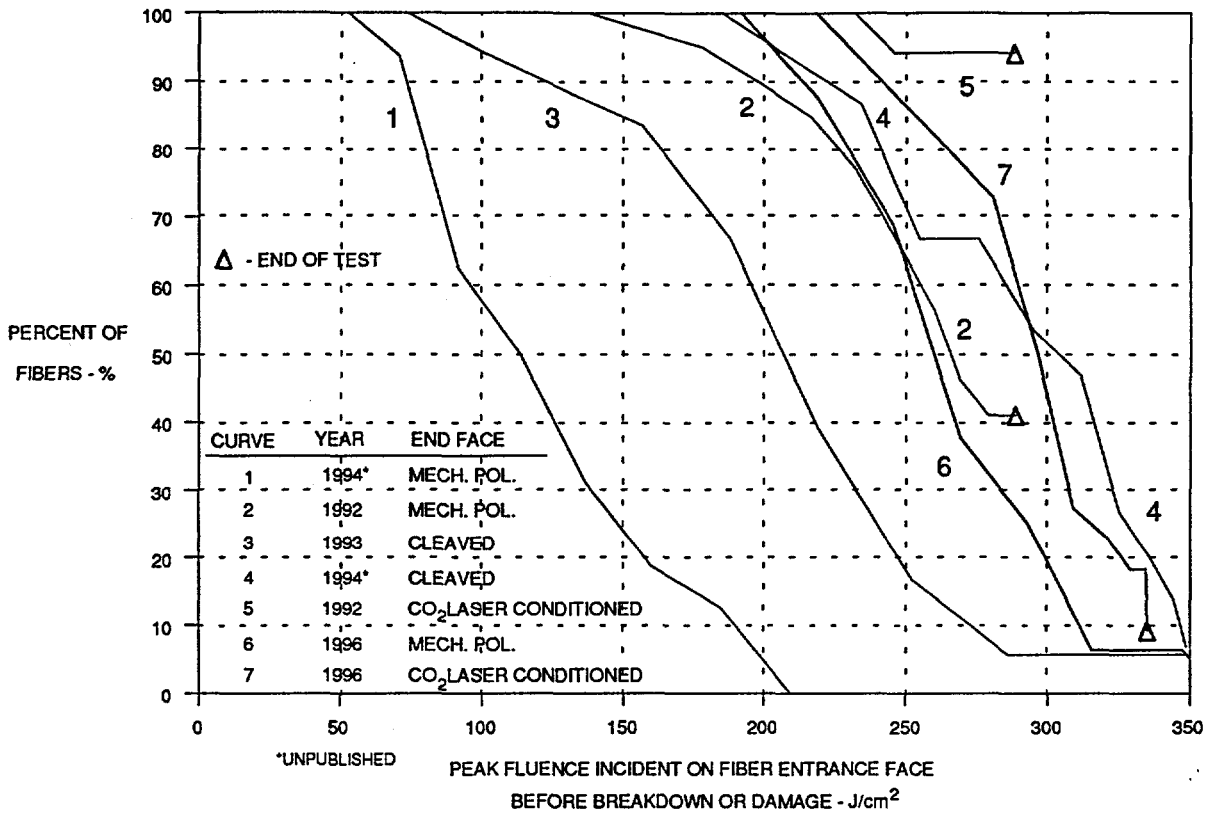

Fig. 16 Comparisons between previous and current (1996) results. The 1992 data used a fiber-to fiber injection method; all other data used a simple lens injection method. The 1994 data in this figure have not been previously reported, and were obtained with fiber having either polished or cleaved end faces as received directly from a commercial vendor.

than is typically used in damage testing of substrates, reducing the relative likelihood of encountering surface defects that have some probability for occurrence per unit area. Consequently, the present results can be biased towards higher thresholds when compared to other reported thresholds that are based on this definition and on "one-on-one" test procedures. With these caveats in mind, we can compare our current results to thresholds reported in terms of peak incident fluence on bare fused-silica surfaces at our wavelength. The most comprehensive testing has been performed at Lawrence Livermore National Laboratory.[18] Using their scaling laws to account for our laser pulsewidth, a nominal threshold value for a range of surface preparations is approximately 60 J/cm^2. For silica samples with superior surface finishes, thresholds were found to rise to nearly 170 J/cm^2 at our pulsewidth. Considering the various reasons why our results may be biased towards higher values, this comparison indicates that our results are consistent with the most representative data available from non-fiber testing.

The value of end-face conditioning with a CO_2 laser is further illustrated by the comparison of damage sites observed in the current study shown in Table 1. Without the end-face conditioning, the results were dominated by entrance-face breakdown at a level that largely preempted other damage mechanisms. With end-face conditioning, higher laser levels were passing beyond the entrance face and eventually triggering other damage processes. A single damage mechanism did not dominate the results, although a majority of fibers damaged either in the "entry" segment or within the 360° loop. Both of these damage processes could be further inhibited if a broader mode power distribution could be generated immediately beyond the fiber entrance face (as was achieved by the fiber-to-fiber injection method). Hopefully, continuing work on diffractive optics will ultimately achieve this goal and eliminate the need for a mechanical mode scrambler in the process. Nevertheless, the fact that the observed damage events were well distributed over the possible damage processes suggests that the current results may be approaching a practical limit for high-intensity laser transmission through fibers.

Table 1. Comparison of damage sites in the current study.

BREAKDOWN/DAMAGE SITE	PRELIMINARY LOT - NO CO_2-LASER CONDITIONING		FIBERS WITH CO_2-LASER CONDITIONING	
	NUMBER OF FIBERS	AVERAGE TRANSMITTED ENERGY BEFORE DAMAGE mJ	NUMBER OF FIBERS	AVERAGE TRANSMITTED ENERGY BEFORE DAMAGE mJ
ENTRANCE FACE	11	74.0	4	85.6
"ENTRY"	1	79.1	6	91.8
MODE SCRAMBLER	3	75.2	1	68.4
360^0 LOOP	0	-	8	86.1
EXIT FACE	1	72.2	1	91.0
NO DAMAGE	0	-	2	104.2
TOTALS:	16	74.4	22	88.9

6. ACKNOWLEDGMENTS

This work was supported by the United States Department of Energy under Contract DE-AC04-94AL85000. Sandia is a multiprogram laboratory operated by Sandia Corporation, a Lockheed Martin Company, for the United States Department of Energy. The author would like to thank Paul Klingsporn of Allied-Signal, Inc., Kansas City Division, for providing the polished fiber samples used in this study. The talented contributions of Dante Berry, Geo-Centers, Inc., Albuquerque, in assembling and operating the CO_2-laser conditioning system, in designing and assembling the current damage testing configuration, and in performing all of the damage tests, were greatly appreciated.

7. REFERENCES

1. K. Rink, G. Delacretaz, and R. P. Salathe, "Fragmentation Process Induced by Microsecond Laser Pulses During Lithotripsy," Appl. Phys. Lett. 61, 258 (1992).

2. J. D. Denstedt, H. A. Razvi, S. S. Chun, and J. L. Sales, "Intracorporeal Lithotripsy with the Holmium:YAG Laser," Proc. SPIE 2395, 89 (1995).

3. D. L. Paisley, R. H. Warnes, and R. A. Kopp, "Laser-Driven Flat Plate Impacts to 100 GPa with Sub-Nanosecond Pulse Duration and Resolution for Material Property Studies," in Shock Waves in Condensed Matter - 1991, S. C. Schmidt, R. D. Dick, J. W. Forbes, and D. G. Tasker, Eds., Elsevier Science Publishers, New York, p. 825 (1992).

4. R. J. Lawrence and W. M. Trott, "Theoretical Analysis of a Pulsed-Laser-Driven Hypervelocity Flyer Launcher," Intl. J. Impact Eng. 14, 439 (1993).

5. L. C. Yang and V. J. Menichelli, "Laser Initiation of Insensitive High Explosives," Proceedings of the Sixth Symposium (International) on Detonation, Office of Naval Research, ACR-221, Arlington, VA, 1976, p. 612.

6. A. M. Renlund, P. L. Stanton, and W. M. Trott, "Laser Initiation of Secondary Explosives," Proceedings of the Ninth Symposium (International) on Detonation, Office of the Chief of Naval Research, OCNR 113291-7, Arlington, VA, 1991, p. 1118.

7. R. E. Setchell, K. D. Meeks, W. M. Trott, P. Klingsporn, and D. M. Berry, "High-Power Transmission Through Step-Index, Multimode Fibers," Proc. SPIE 1441, 61 (1991).

8. R. E. Setchell and P. Klingsporn, "Laser-Induced Damage Studies on Step-Index, Multimode Fibers," Proc. SPIE 1624, 56 (1992).

9. R. E. Setchell, "Laser-Induced Damage in Step-Index, Multimode Fibers," Proc. SPIE 1848, 15 (1993).

10. R. E. Setchell, "Damage Studies in High-Power Fiber Transmission Systems," Proc. SPIE 2114, 87 (1994).

11. R. E. Setchell, "Reduction in Fiber Damage Thresholds Due to Static Fatigue," Proc. SPIE 2428, 54 (1995).

12. D. Gloge, "Optical Power Flow in Multimode Fibers," Bell Syst. Tech. J. 51, 1767 (1972).

13. S. W. Allison, G. T. Gillies, D. W. Magnuson, and T. S. Pagano, "Pulsed Laser Damage to Optical Fibers," Appl. Opt. 24, 3140 (1985).

14. R. Pini, R. Salimbeni, and M. Vannini, "Optical Fiber Transmission of High Power Excimer Laser Radiation," Appl. Opt. 26, 4185 (1987).

15. W. M. Trott and K. D. Meeks, "High-Power Nd:Glass Laser Transmission Through Optical Fibers and Its Use in Acceleration of Thin Foil Targets," J. Appl. Phys. 67, 3297 (1990).

16. A. W. Snyder and J. D. Love, Optical Waveguide Theory, Chapman and Hall, London, 1983, pp.180-188.

17. N. L. Boling, M. D. Crisp, and G. Dube, "Laser Induced Surface Damage," Appl. Opt. 12, 760 (1973).

18. F. Ranier, L. J. Atherton, J. H. Campbell, F. D. De Marco, M. R. Kozlowski, A. J. Morgan, and M. C. Staggs, "Four-Harmonic Database of Laser-Damage Testing," Proc. SPIE 1624, 116 (1992).

19. J. D. Crow, "Power Handling Capability of Glass Fiber Lightguides," Appl. Opt. 13, 467 (1974).

20. For example, see : D. E. Quinn, "Optical Fibers," in Fiber Optics Handbook, F. C. Allard, Ed., McGraw-Hill, New York, 1990, pp. 1.39-1.42.

21. P. A. Temple, W. H. Lowdermilk, and D. Milam, "Carbon Dioxide Laser Polishing of Fused Silica Surfaces for Increased Laser-Damage Resistance at 1064 nm," Appl. Opt. 21, 3249 (1982).

22. A. J. Weber, A. F. Stewart, G. J. Exarhos, and W. K. Stowell, "An Investigation of Laser Processing of Silica Surfaces," Laser Induced Damage in Optical Materials: 1986, National Institute of Standards and Technology Special Publication 752, p. 542, 1988.

23. B. Bergman, "On the Estimation of the Weibull Modulus," J. Mater. Sci. Lett. 3, 689 (1984).

24. For example, see: C. R. Wolfe, M. R. Kozlowski, J. H. Campbell, F. Rainer, A. J. Morgan, and R. P. Gonzales, "Laser Conditioning of Optical Thin Films," Laser Induced Damage in Optical Materials: 1989, National Institute of Standards and Technology Special Publication 801, p. 360, 1990. Also: references cited within.